

Effects of air loading on the acoustics of an Indian musical drum

Sankalp Tiwari and Anurag Gupta^{a)}

Department of Mechanical Engineering, Indian Institute of Technology, Kanpur 208016, India

(Received 7 May 2016; revised 23 March 2017; accepted 24 March 2017; published online 12 April 2017)

The effects of air loading on the acoustical properties of tabla, an Indian musical drum, are investigated by idealizing it as a composite membrane backed by a rigid cylindrical cavity. The coupled boundary value problem for membrane vibration and acoustic pressure, assuming acoustic radiations to be the only source of dissipation, is solved using a Green's function method. It is shown that air loading helps in only fine tuning of the harmonicity of the composite membrane in the right hand tabla, but significantly improves the harmonicity in the left hand tabla. In both cases, it increases the decay time of the musically important modes. With a suitably defined error as the objective function, optimum tabla designs are found, which yield the most harmonic frequency spectrum. The obtained results are found to be consistent with the actual design of the tabla. Modal sound synthesis of the percussion instrument has also been attempted. © 2017 Acoustical Society of America. [<http://dx.doi.org/10.1121/1.4979782>]

[MAH]

Pages: 2611–2621

I. INTRODUCTION

It is well known that the natural frequencies of an ideal circular membrane are inharmonic. A composite circular membrane, with added mass in a central radially symmetric region, can, however, yield five approximately harmonic frequencies distributed over nine modes.^{1,2} Of course, such harmonicity is approached only for carefully chosen values of density and radius ratios of the added mass to the base membrane.^{2,3} The fundamental is from 01 mode, the second harmonic from 11 mode, the third from 21 and 02 modes, the fourth from 31 and 12 modes, and the fifth harmonic from 41, 03, and 22 modes. On the other hand, a composite membrane with an eccentrically located region of extra mass does not yield harmonic overtones.⁴ The inharmonicity of the ideal membrane can alternatively be (partially) removed by incorporating air loading and a suitably sized cavity backing the membrane; this is well understood in the context of kettledrum.^{5,6}

The present work is motivated by the lack of detailed investigations into the effects of coupling air loading and cavity with the composite membrane, both with central and eccentric mass distribution. Such considerations are required to understand the acoustics of tabla, a popular Indian drum with a strong sense of pitch. A preliminary study towards this end was initiated by Bhat⁷ who assumed the pressure due to air cavity to be uniform over the membrane and hence predicted a change only in the axisymmetrical modes. More recently, an attempt has been made, in an unpublished master's thesis,⁸ to use a Green's function method to incorporate air loading with the symmetrically loaded membrane. The relevant discussion in the thesis is very brief, without any mention of the decay rates, optimization of design, and application to the eccentric loading case. Moreover, there is an error in the frequencies reported for the 41 mode. Our

aim is to fill these gaps by presenting a rigorously developed model which incorporates the presence of both the ambient air, surrounding the composite membrane, and the enclosed air within a rigid cavity backing the membrane. We find, confirming experimental observations,^{1,2} that the additional consideration of air loading improves the harmonicity of composite membranes as well as sustain the musically important modes longer than the other modes. We also use our model to determine optimum designs of cavity backed composite membranes, in a suitable geometric and material space, which maximize the harmonicity in the frequency spectrum. The optimization results again confirm the prevailing design practices among tabla makers. Finally, we present a framework for modal sound synthesis of the percussion instrument with an aim of moving a step closer to digitally reconstructing tabla sounds.

Tabla consists of a treble drum (right hand tabla) and a bass drum (left hand tabla), both played horizontally with hands (see Fig. 1).^{9,10} The right hand tabla is carved out of a single cylindrical block of wood (generally Indian Rosewood), around 0.2 m in height and 0.05 m in radius, hollowed on one end to almost half of the total height of the shell. The depth of the hollow part is kept short enough to prevent warping and long enough to avoid an unnecessarily heavy shell.¹⁰ The hollow shell of the left hand tabla is instead made of either clay or metal (brass, copper, steel, or aluminium); it is approximately 0.25 m high and has a drumhead of radius around 0.10 m. Both parts of tabla are closed at the bottom. The iconic feature of tabla design is its drumhead composed of a layer of goat hide covered with another layer which is trimmed so as to form a rim around the first layer (see Fig. 1). The trimmed layer, helpful in dampening out the inharmonic higher modes (conjectured by Raman¹), will not be considered in the present study. Additional mass is distributed over the drumhead, centrally in the right hand tabla and eccentrically in the left hand tabla, in a radially symmetric region of around 0.025 m in radius. The additional mass,

^{a)}Electronic mail: ag@iitk.ac.in



FIG. 1. (Color online) The left hand and the right hand tabla.

made of a black paste of iron (or stone) powder mixed with wheat flour dough, appears on the drumhead as a black patch (also called *siyāhī*). The two skin layers in the composite drumhead are laced to a ring and are tightened/attached to the drum shell using straps of buffalo hide. The right hand tabla is tunable using the wooden pegs inserted between the shell and the straps (see Fig. 1) and also by gently stroking the edge of the drumhead with a hammer. Once tabla is tuned, its acoustical richness can be gauged by certain fundamental strokes (two of which are described in Sec. 1.1 of the supplementary material).^{9,11,12} It is commonly observed that the fundamental of the right hand tabla is raised by more than ten percent. This is often desirable by the tabla players.^{11,13} The harmonic overtones can be heard, for instance, when a player rests his ring finger lightly on the edge of the black patch (of the right tabla) and strikes the outer halo with his index finger. This stroke (called *nā*) has a dominant contribution from the second and third harmonic as the lightly pressed ring finger keeps out the fundamental mode.¹¹ The left hand tabla, tuned one octave below the right hand tabla, gives a bassy texture to the overall sound. The overtones of the left tabla are also found to be in harmonic relationship with its fundamental.¹¹

In the present work we idealize the right hand tabla as a composite membrane, with a central region of additional mass, backed by a rigid cylindrical cavity. The coupled boundary value problem includes the standard transverse vibration equation for a circular membrane, but with piecewise constant density and air loading, and acoustics wave equation for pressure. An infinite rigid baffle is assumed to occupy the membrane plane outside the drum. A Green's function method, following an earlier work on kettledrum by Christian *et al.*,^{6,8} is then used to solve for modal frequencies. The left hand tabla, on the other hand, is modelled as an ideal membrane (of uniform density) of radius and density of the region with the additional mass (the black patch) backed by a rigid cylindrical cavity, but bounded by an elastic support with varying stiffness. The unconfined air mass above the membrane lowers the frequency of all modes of membrane vibration, while the enclosed air in the cavity stiffens the membrane and increases the frequency of the axisymmetric modes. The respective problems, and solution methodologies, for the right and the left hand tabla are given in Secs. II A and II B. These solutions are used in Sec. III A to find optimal designs of the right hand tabla in a six-dimensional parametric

space which includes spatial dimensions, tension in the membrane, and density values. In particular, we note that there is a considerable latitude in choosing the parameters which ensure experimentally observed harmonicity of tabla. This is consistent with the practice of tabla making.¹⁰ For optimal parameters, the resulting frequency spectrum and decay times are explored in Secs. III B and III C, respectively. In Secs. III D and III E, we revisit these issues for left hand tabla. Finally, in Sec. III F, we present some results from the modal sound synthesis of tabla. The details of synthesis technique are given in the accompanying supplementary material.¹² The supplementary document also contains experimentally obtained frequency spectrums of two major tabla strokes and some additional results from the optimization analysis. We conclude our paper in Sec. IV with some open directions for future research.

II. PROBLEM FORMULATION AND SOLUTION METHODOLOGY

Idealizing both right and left hand tabla as cylindrical cavity backed circular membranes, we now pose coupled boundary value problems for membrane vibration and air pressure distribution. We also extend an existing Green's function method⁶ to solve the problem to obtain natural frequencies and decay times of the cavity backed composite membranes.

A. Right hand tabla

Consider a composite membrane fixed at the edge, as shown in Fig. 2(a), which is allowed to vibrate in the transverse direction while being stretched by a uniform tension T . The air pressure loads the membrane from outside, due to the ambient atmosphere, and from inside, due to the closed cylindrical cavity. With respect to a cylindrical coordinate system (ρ, ϕ, z) , see Fig. 2(a), the transverse motion $\eta(\rho, \phi, t)$ (t denotes time) of the membrane (located at $z = L$) is governed by

$$\sigma(\rho) \frac{\partial^2 \eta}{\partial t^2} = T \left[\frac{1}{\rho} \frac{\partial}{\partial \rho} \left(\rho \frac{\partial \eta}{\partial \rho} \right) + \frac{1}{\rho^2} \frac{\partial^2 \eta}{\partial \phi^2} \right] + p(\rho, \phi, L_-, t) - p(\rho, \phi, L_+, t), \quad (1)$$

where $\sigma(\rho)$ is the areal density of the membrane having piecewise constant values, σ_1 for $0 \leq \rho \leq a$ and σ_2 for $a < \rho \leq b$, and p is the acoustic pressure field. In the arguments of the latter, L_- (L_+) represents the limiting value of the transverse direction as it approaches the membrane from inside (outside) the cavity. The inner density is assumed to be more than the outer density, i.e., $\sigma_1 > \sigma_2$. More sophisticated density distributions were considered recently.³ Note that pressure p is unknown and has to be solved using another boundary value problem as discussed below. Let η_1 and η_2 be the value of η over $0 \leq \rho \leq a$ and $a < \rho \leq b$, respectively. The boundary conditions to be satisfied by η_1 and η_2 are

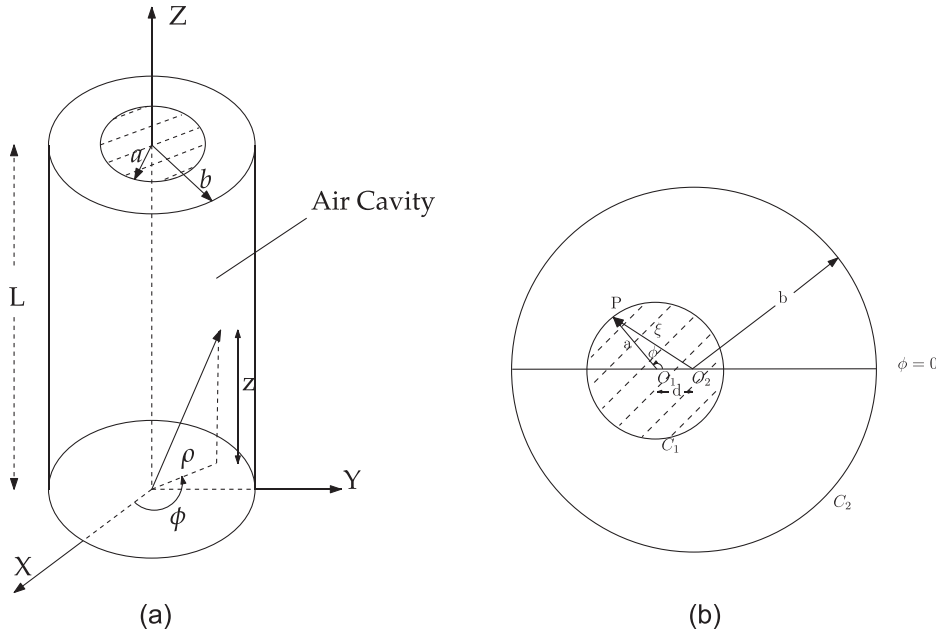


FIG. 2. (a) The right tabla as a composite membrane backed by cylindrical cavity. (b) Top view of the left tabla membrane.

$$\eta_1(a, \phi, t) = \eta_2(a, \phi, t), \quad \frac{\partial \eta_1}{\partial \rho}(a, \phi, t) = \frac{\partial \eta_2}{\partial \rho}(a, \phi, t), \quad (2)$$

$$\eta_2(b, \phi, t) = 0, \quad \text{and} \quad (3)$$

$$\eta_i(\rho, \phi, t) = \eta_i(\rho, \phi + 2n\pi, t), \quad \text{for } i = 1, 2. \quad (4)$$

The conditions in Eq. (2) impose continuity of displacement and traction at the interface of the two domains, Eq. (3) is the consequence of membrane being fixed at the edge, and Eq. (4) ensures that displacement remain single valued. We also require η_1 and η_2 to remain finite over the membrane. The eigenfunctions satisfying these boundary conditions are given in Appendix A.

The acoustic pressure $p(\rho, \phi, z, t)$ satisfies the wave equation

$$\left(\Delta - \frac{1}{c_a^2} \frac{\partial^2}{\partial t^2} \right) p = 0, \quad (5)$$

where c_a is the speed of sound in air and Δ is the Laplacian operator. Assuming the walls of the cavity to be perfectly rigid, we require

$$\frac{\partial p}{\partial \rho}(b, \phi, z, t) = \frac{\partial p}{\partial z}(\rho, \phi, 0, t) = 0 \quad (6)$$

for the internal pressure. As for the outside pressure, we assume that an infinite rigid baffle surrounds the membrane in the $z=L$ plane requiring⁶

$$\frac{\partial p}{\partial z}(\rho, \phi, L, t) = 0 \quad \forall \rho > b. \quad (7)$$

The presence of baffle has been shown to have only a moderate effect on the results;⁶ its incorporation, however, greatly simplifies the analytical calculation. Overall, Eqs. (1)–(7) form a coupled boundary value problem for transverse

displacement and pressure. We assume both transverse displacement and pressure to have harmonic time dependence, i.e., $\eta(\rho, \phi, t) = \eta(\rho, \phi)e^{i\omega t}$ and $p(\rho, \phi, z, t) = p(\rho, \phi, z)e^{i\omega t}$.

The internal and external pressure acting on the membrane can be calculated using Green functions G_{in} and G_{out} , whose expressions are given in Appendix B, as⁶

$$p(\rho, \phi, L_-) = \frac{1}{4\pi} \int_0^b \rho' d\rho' \int_0^{2\pi} d\phi' G_{\text{in}}(\rho, \phi, L_- | \rho', \phi', L) \times \frac{\partial p}{\partial z'}(\rho', \phi', L_-) \quad (8)$$

and

$$p(\rho, \phi, L_+) = -\frac{1}{4\pi} \int_0^b \rho' d\rho' \int_0^{2\pi} d\phi' G_{\text{out}}(\rho, \phi, L_+ | \rho', \phi', L) \times \frac{\partial p}{\partial z'}(\rho', \phi', L_+). \quad (9)$$

The pressure gradient appearing in the integrands above can be replaced by η using $\rho_0 \omega^2 \eta(\rho, \phi) = (\partial p / \partial z)(\rho, \phi, L)$, where ρ_0 is the equilibrium density of air. Expanding η in terms of basis functions provided by the normal modes of the composite membrane without air loading (given in Appendix A), (1) yields

$$\begin{aligned} & -a_{ns}^m \left(\omega^2 - \frac{X_{mn}^2}{b^2} c_2^2 \right) \left[\sigma_1 \int_0^a \int_0^{2\pi} \eta_{1mn}^0 \eta_{1mn}^0 \rho d\phi d\rho \right. \\ & \quad \left. + \sigma_2 \int_a^b \int_0^{2\pi} \eta_{2mn}^0 \eta_{2mn}^0 \rho d\phi d\rho \right] \\ & = \rho_0 \omega^2 \sum_{n''=1}^{\infty} a_{n''s}^m U_{nn''} + \rho_0 \omega^2 \sum_{n''=1}^{\infty} a_{n''s}^m V_{nn''}, \end{aligned} \quad (10)$$

where $U_{nn''}$ and $V_{nn''}$ are as given in Appendix B. The above equation can be solved iteratively for ω . As a first

approximation, ω is taken as $X_{mn}c_2/b$ (see Appendix A for the definitions of X_{mn} and c_2). Restricting both n and n'' to vary from one to five, we find solutions converging readily. At the end of each iteration, that value of ω which corresponds to the mode with s nodal circles is selected and substituted back in $U_{nn''}$ and $V_{nn''}$. The process is repeated until the values of successive frequencies agree to at least two decimal places. The frequency ω has a real and an imaginary part:

$$\omega = \omega_{mn} + i\omega_i. \quad (11)$$

The subscripts m and n in the real part ω_{mn} indicate m diametrical nodes and n circular nodes. The imaginary part ω_i is related to the decay time of the (mn) th mode. The 60-dB decay time (t_{60}), which is the time for the pressure amplitude to decay to 1/1000 times its initial value, is given by

$$t_{60} = 3/(\omega_i \log e), \quad (12)$$

where \log should be understood as the logarithm with base 10. This relation is easily derived starting from $p = p_0 e^{i\omega t}$. The pressure amplitude at initial time is p_0 whereas at time t it is given by $p_0 e^{-\omega_i t}$. If the latter is 1000 times smaller than p_0 then we require $e^{\omega_i t} = 1000$. Taking a logarithm we obtain the required relation.

We have used a methodology similar to that used previously for kettledrum.⁶ There are, however, two notable differences. The basis functions η^0 for the transverse displacement are more involved since they are obtained for a composite membrane. Second, we are always required to separate the two domains while performing integrations over the membrane surface.

B. Left hand tabla

The left hand tabla is the bigger of the two pieces and serves as the bass drum owing to its low natural frequencies. Unlike the right hand tabla, it lacks circular symmetry due to the eccentrically placed loaded patch. Following Ramakrishna,⁴ rather than working with a composite membrane, we will treat the drumhead as a membrane having radius and density of the loaded region, and stretched to the same tension, but having a transverse elastic support all along the boundary with a stiffness which varies with ϕ . An alternate solution for composite membranes with eccentric loading was proposed by Sarojini and Rahman,¹⁴ who used a variational method with bipolar coordinate system, without making any other simplifications. Their solution is however difficult to implement and is valid only for small eccentricities.

Figure 2(b) shows an idealized representation of the top view of the left tabla membrane. Here, O_1 and O_2 are the centres of the loaded patch of radius a and the complete membrane of radius b , respectively. The distance between the two centres is d . We assume stiffness to be of the form⁴

$$k(\phi) = \frac{A}{\log[b/\xi(\phi)]}, \quad (13)$$

where $\xi(\phi) = (a^2 + d^2 - 2ad \cos \phi)^{1/2}$ is the distance of a point P on the boundary of the loaded patch from O_2 . To solve for constant A , we consider quasi-static deformation of a circular membrane of radius a stretched with tension T and acted upon by a force per unit length F at $\rho = a$ and a uniform pressure \tilde{p} . The equation of force balance takes the form

$$T \frac{1}{\rho} \frac{\partial}{\partial \rho} \left(\rho \frac{\partial \eta(\rho)}{\partial \rho} \right) = -F \delta(\rho - a) - \tilde{p}. \quad (14)$$

Assuming adiabatic expansion, it is easy to show that

$$\tilde{p} = -\frac{2\pi\gamma p_0}{V_0} \int_0^b \eta(\rho) d\rho, \quad (15)$$

where γ is the specific heat constant of air, p_0 the initial pressure, and V_0 the initial volume. This integral equation can be solved for displacement at $\rho = a$:

$$\eta(a) = \frac{aF}{T} \left[\ln\left(\frac{b}{a}\right) - \frac{\gamma p_0 (b^2 - a^2)^2}{8b^2 LT \left(1 + \frac{\gamma p_0 b^2}{8LT}\right)} \right]. \quad (16)$$

The ratio $F/\eta(a)$ can now be evaluated to obtain A .

The normal modes for the circular membrane as considered above, but without the cavity, are given by

$$\begin{aligned} \eta_{emn}^0(\rho, \phi) &= J_m(\zeta'_{emn}\rho) \cos m\phi, \\ \eta_{omn}^0(\rho, \phi) &= J_m(\zeta'_{omn}\rho) \sin m\phi, \end{aligned} \quad (17)$$

where

$$\begin{aligned} \zeta_{emn}^2 &= \left(\frac{X_{mn}}{a}\right)^2 + \frac{2\beta^2 X_{mn}^2}{\pi a^2 (X_{mn}^2 + \beta^2 - m^2)} \int_0^{2\pi} \ln\left(\frac{\xi(\phi)}{a}\right) \\ &\times \left(1 - \frac{\gamma p_0 (b^2 - a^2)^2}{8b^2 LT \ln\left(\frac{b}{a}\right) \left(1 + \frac{\gamma p_0 b^2}{8LT}\right)}\right) \\ &\times \cos^2 m\phi d\phi \quad \text{and} \\ \zeta_{omn}^2 &= \left(\frac{X_{mn}}{a}\right)^2 + \frac{2\beta^2 X_{mn}^2}{\pi a^2 (X_{mn}^2 + \beta^2 - m^2)} \int_0^{2\pi} \ln\left(\frac{\xi(\phi)}{a}\right) \\ &\times \left(1 - \frac{\gamma p_0 (b^2 - a^2)^2}{8b^2 LT \ln\left(\frac{b}{a}\right) \left(1 + \frac{\gamma p_0 b^2}{8LT}\right)}\right) \\ &\times \sin^2 m\phi d\phi. \end{aligned} \quad (18)$$

The subscripts e and o correspond to the even and odd displacement functions, respectively. The term X_{mn} is the n th root of the equation

$$J'_m(X)/J_m(X) = -\beta/X, \quad (19)$$

where $\beta = Aa/[T \ln(b/a)]$.

We can now proceed in exactly the same manner as was done in the case of right hand tabla. The displacement functions for the membrane subjected to air loading can be expanded in terms of Eq. (17) and substituted into the governing equation

$$\begin{aligned}
& -[\sigma_1 \omega^2 \eta(\rho, \phi) + T \Delta \eta(\rho, \phi)] \\
& = p(\rho, \phi, L_-) - p(\rho, \phi, L_+), \tag{20}
\end{aligned}$$

where σ_1 is the areal density of the loaded patch and harmonic time dependence is assumed. The governing equation for natural frequencies takes the form

$$\begin{aligned}
& -a_{ns}^m \left(\omega^2 - \frac{X_{mn}^2}{a^2} c_1^2 \right) \sigma_1 \int_0^a \int_0^{2\pi} \eta_{emn}^0 \eta_{emn}^0 \rho d\phi d\rho \\
& = \rho_0 \omega^2 \sum_{n''=1}^{\infty} a_{n''s}^m U_{nn''} + \rho_0 \omega^2 \sum_{n''=1}^{\infty} a_{n''s}^m V_{nn''}
\end{aligned}$$

or

$$\begin{aligned}
& -a_{ns}^m \left(\omega^2 - \frac{X_{mn}^2}{a^2} c_1^2 \right) \sigma_1 \int_0^a \int_0^{2\pi} \eta_{omn}^0 \eta_{omn}^0 \rho d\phi d\rho \\
& = \rho_0 \omega^2 \sum_{n''=1}^{\infty} a_{n''s}^m U_{nn''} + \rho_0 \omega^2 \sum_{n''=1}^{\infty} a_{n''s}^m V_{nn''}, \tag{21}
\end{aligned}$$

where $c_1 = \sqrt{T/\sigma_1}$, whichever the case may be. The expressions for $U_{nn''}$ and $V_{nn''}$ for the even case are given by

$$\begin{aligned}
U_{nn''} & = \frac{1}{4\pi} \int_0^a \int_0^{2\pi} \int_0^a \rho' d\rho' \\
& \times \int_0^{2\pi} d\phi' G_{in}(\rho, \phi, L_- | \rho', \phi', L) \\
& \times \eta_{emn''}^0(\rho', \phi') \eta_{emn}^0(\rho, \phi) \rho d\phi d\rho, \tag{22}
\end{aligned}$$

$$\begin{aligned}
V_{nn''} & = \frac{1}{4\pi} \int_0^a \int_0^{2\pi} \int_0^a \rho' d\rho' \\
& \times \int_0^{2\pi} d\phi' G_{out}(\rho, \phi, L_+ | \rho', \phi', L) \\
& \times \eta_{emn''}^0(\rho', \phi') \eta_{emn}^0(\rho, \phi) \rho d\phi d\rho. \tag{23}
\end{aligned}$$

The respective expressions for the odd case can be written likewise.

III. RESULTS AND DISCUSSION

We have divided our results into six subsections. First, we look for optimum designs of the cavity backed composite membrane so as to mimic the harmonicity and degeneracy of overtones as observed experimentally for the right hand tabla.^{1,2} Second, we discuss in detail the variation of harmonic frequencies of the composite membrane due to air loading and the air column in the cavity. We also investigate the variation in frequencies for differently tuned drums, supplemented with some experimental observations to support our discussion. Next, we use our model to estimate the decay times and study the sustainability of different modes as the

energy is radiated away due to air damping. Following these, we revisit the issues of harmonic frequencies, decay rates, and optimum designs for the left hand tabla. In particular, we find greater harmonicity due to the air column than what is otherwise reported in previous theoretical investigations. Finally, we present some results from the modal sound synthesis, leaving out the details to the supplement.

A. Optimal design of right hand tabla

For investigating the design of the right hand tabla, we consider the following six parameters: outer density (σ_2), ratio of inner density to outer density (λ^2), outer radius (b), ratio of inner radius to outer radius (k), tension per unit length in the membrane (T), and length of the air column within the cavity (L). For every fixed set of value of these parameters we can obtain the first nine natural frequencies associated with the cavity backed composite membrane structure, and subsequently calculate the error function

$$\begin{aligned}
& E(\sigma_2, \lambda, b, k, T, L) \\
& = \frac{8}{13} \left(\frac{2\omega_{01}/\omega_{11} - 1.1}{1.1} \right)^2 + \frac{16}{13} \left(\frac{2\omega_{02}/\omega_{11} - 3}{3} \right)^2 \\
& + \frac{16}{13} \left(\frac{2\omega_{21}/\omega_{11} - 3}{3} \right)^2 + \frac{16}{13} \left(\frac{2\omega_{12}/\omega_{11} - 4}{4} \right)^2 \\
& + \frac{16}{13} \left(\frac{2\omega_{31}/\omega_{11} - 4}{4} \right)^2 + \frac{8}{13} \left(\frac{2\omega_{03}/\omega_{11} - 5}{5} \right)^2 \\
& + \frac{8}{13} \left(\frac{2\omega_{22}/\omega_{11} - 5}{5} \right)^2 + \frac{8}{13} \left(\frac{2\omega_{41}/\omega_{11} - 5}{5} \right)^2. \tag{24}
\end{aligned}$$

In formulating the above error function, we have used various experimentally established acoustic features of the right hand tabla. Following Raman,¹ we have considered only the first nine modes as the higher modes damp out quickly due to the annular rim surrounding the composite membrane. Second, the ratio of fundamental frequency to that of the 11 mode is measured to be 1.10/2.^{2,11} This inharmonicity is psychoacoustically preferred as it allows us to hear a lower fundamental than what the tabla is able to produce.¹³ Third, we recognize the experimental observation that modes 02 and 21, 12 and 31, and 03, 22, and 41 are degenerate.¹ Finally, we have ascribed higher weight functions for these modes to come into a harmonic relationship since there are generally accepted to be musically important modes in comparison to others. All these features in the proposed error function have been incorporated with an intention to come up with a most optimum design of right hand tabla in the six-dimensional parametric space.

The optimization problem is to minimize the error function (24) in a suitably chosen closed subset of the six-dimensional parametric space. Towards this end, we have used Matlab's Genetic Algorithm optimization toolbox. Interestingly, we find the error value to be little sensitive to perturbations around the minimum, suggesting a wide flat valley surrounding the minimum. This can be seen from the three plots in Figs. 3(a), 3(b), and 3(c) (similar figures

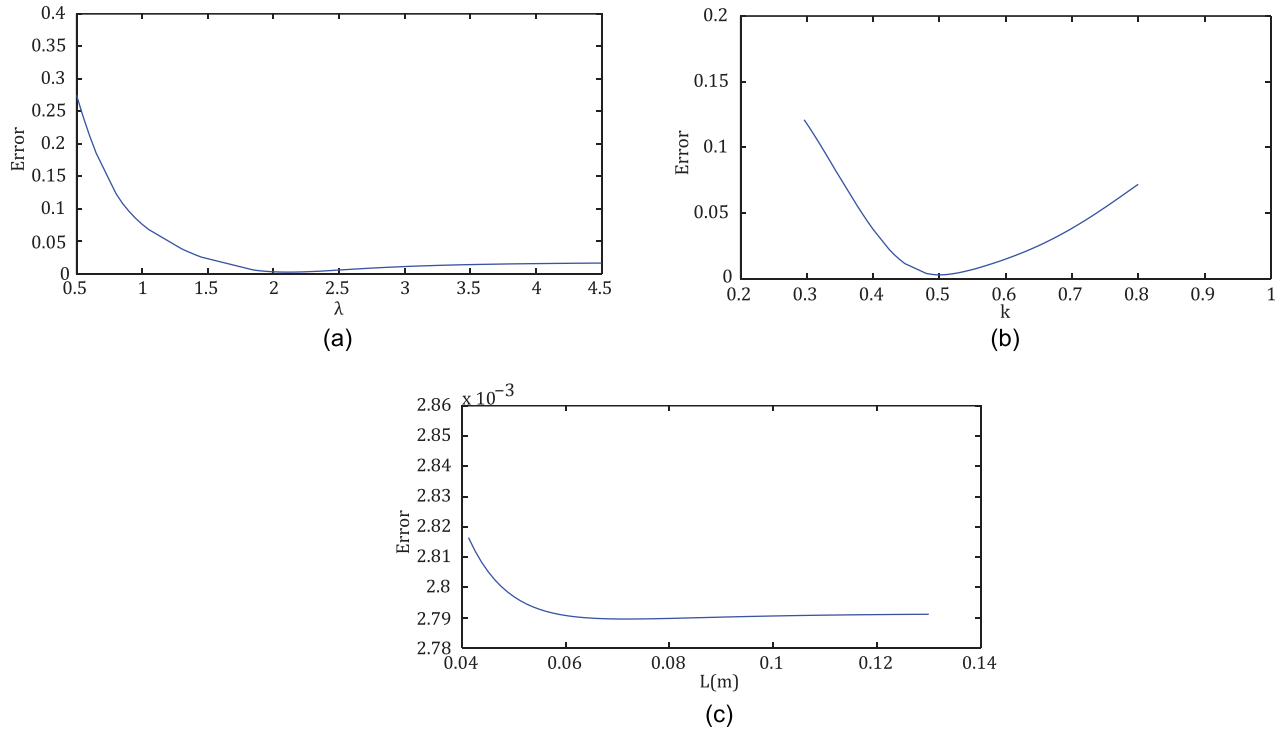


FIG. 3. (Color online) Error function under variation of parameters. The remaining parameters in each of the above plots are fixed as given in the first row of Table I.

plotted with respect to other parameters are given in Sec. 3 of the supplementary material¹²). This valley has a somewhat sharper gradient in the k -direction. We have provided six combinations of various parameters, with corresponding fundamental frequency and error value, in Table I. The error sensitivity to variations in k is clearly seen in this table. For presentation of our results we fix $L = 0.1$ m, although the error function is minimized for values of L around 0.072 m, so as to be closer to actual dimensions of the right tabla. Our choice of L introduces very little change in error, as can be seen from Fig. 3(c).

We note from Table I that low error values can correspond to a wide range of the outer radius, almost from 0.03 to 0.08 m. Even in practice, one finds a large variety of right hand tablas: small ones with outer radius around 0.05 m to large ones with outer radius around 0.08 m.¹⁵ The length of the air column can take any value above 0.06 m without affecting the harmonicity of the tabla, see Fig. 3(c). This is unlike other parameters which belong to an interval for

yielding low error values. Our model also predicts high harmonicity for a large range of tension values, including the ones which yield practically observed fundamental frequencies (more about tension in Sec. III B). We can safely conclude from our study that, in confirmation with practice of tabla making, there is great leeway in constructing a tabla with a strong sense of pitch.¹⁵

We recall that Ramakrishna and Sondhi² used $\lambda = 3.125$ and $k = 0.4$ in order to calculate frequency ratios for the ideal composite membrane. The error for these values comes out to be 0.0045, higher than almost all of the cases discussed in Table I. On the other hand, Gaudet *et al.*¹⁶ obtained $\lambda = 2.9$ and $k = 0.38$ (corresponding error is 0.0021) as the most optimum parameters for the ideal composite membrane. Their calculation was however based on identifying 03 mode with the sixth harmonic. This is not what is observed experimentally, where this mode is found closer to the fifth harmonic.² In another work, Sathej and Adhikari³ have obtained the optimum values as $\lambda = 2.57$ and $k = 0.492$, again without any considerations of air loading.

Finally, in order to understand the sensitivity of our optimization results with respect to the number of modes considered in the error function, we provide error variations with respect to radius ratio (k) and density ratio (λ) for different cases in Fig. 4. For instance, the blue lines in the plots represent error variation when the error function consists of only the first term in Eq. (24) (with appropriate scaling). The red lines are plots when error function has only the first three terms from Eq. (24), and so on. It is clear that the differences are significant. The optimum λ values get closer to 2 (as is expected from the actual construction of tabla) only when all the nine modes are considered. The k values are also more

TABLE I. Parameter values at the minimum value of the Error function ($L = 0.1$ m). The density σ_2 is given in Kg/m^2 , outer radius of the membrane b in m, and tension T in N/m.

| Parameters ($\sigma_2, \lambda, b, k, T$) | Fundamental frequency (Hz) | Error (E) |
|---|----------------------------|---------------|
| (0.2451, 2.0467, 0.0501, 0.5055, 1821.54) | 356.66 | 0.00279 |
| (0.35, 2.0467, 0.0501, 0.5055, 1821.54) | 360.18 | 0.00303 |
| (0.2451, 2.2, 0.0501, 0.5055, 1821.54) | 469 | 0.00302 |
| (0.2451, 2.0467, 0.08, 0.5055, 1821.54) | 219.91 | 0.00297 |
| (0.2451, 2.0467, 0.0501, 0.65, 1821.54) | 329.98 | 0.0252 |
| (0.2451, 2.0467, 0.0501, 0.5055, 3500) | 494.57 | 0.00313 |

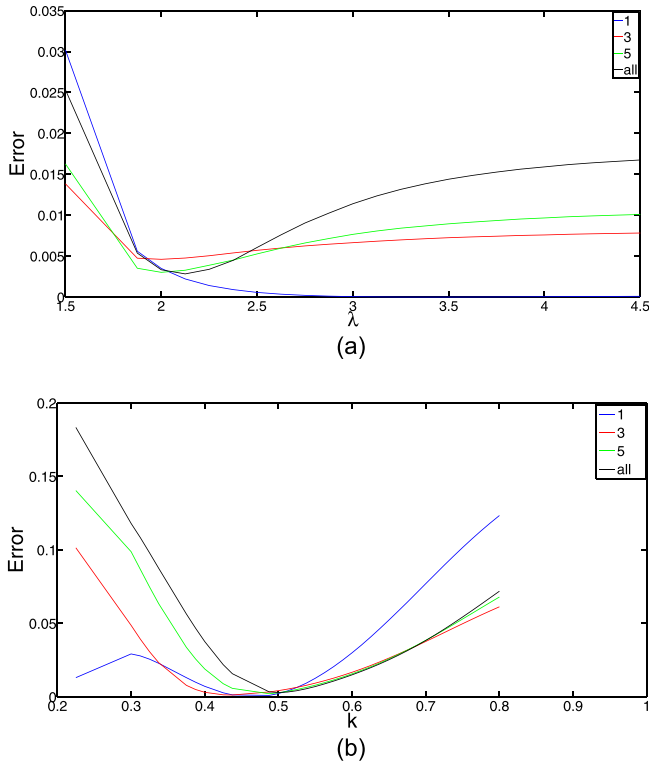


FIG. 4. (Color online) Error function, for varying λ and k , by choosing only few modes for calculating error function of the right hand tabla. The term “all” in the legend refer to all the nine modes as obtained in our computations. The number in the legend denotes the number of modes considered in calculating the error.

tightly bounded around 0.5 when more modes are considered. Similar comparisons can be made with respect to other parameters.

B. Frequency ratios for the right hand tabla

Using the parametric values from the first row of Table I, we obtain the frequency ratios (with respect to the second mode) for the first nine modes in Table II. These are also compared to the values obtained without the enclosed cavity (i.e., membrane in a sea of air), and also with ideal composite

TABLE II. Frequency ratios for the right hand tabla. The value of parameters is as given in the first row of Table I. Only those variables, which appear in the third row above, are needed for the calculations pertaining to the respective column.

| Mode | Uniform membrane | Ideal composite membrane λ, k | Composite membrane without air cavity $\lambda, k, b, \sigma_2, T$ | Composite membrane with air cavity $\lambda, k, b, \sigma_2, T, L$ |
|-------------|------------------|---------------------------------------|--|--|
| η_{01} | 1.26 | 1.12 | 1.09 | 1.12 |
| η_{11} | 2 | 2 | 2 | 2 |
| η_{02} | 3.02 | 3.08 | 3.11 | 3.10 |
| η_{21} | 2.69 | 2.93 | 2.95 | 2.95 |
| η_{12} | 3.67 | 4.04 | 4.12 | 4.02 |
| η_{31} | 3.33 | 3.88 | 3.94 | 3.94 |
| η_{03} | 4.53 | 4.84 | 4.85 | 4.91 |
| η_{22} | 4.40 | 4.95 | 5.05 | 4.94 |
| η_{41} | 3.97 | 4.86 | 4.95 | 4.95 |

membrane and the uniform membrane. It is clear that the shift towards harmonicity of natural frequencies is mainly due to the composite nature of the tabla membrane. The role of air loading is primarily to fine tune the harmonicity between the first nine modes. Further fine tuning is expected if one considers bending stiffness of the membrane.⁵ The role of air loading in achieving harmonicity of Indian drums is minor compared to that in kettledrum. For the kettledrum, an appropriate air loading is crucial to achieve near harmonicity in the first few modes.⁶ As with the kettledrum, the presence of air loading (without the cavity) lowers the frequency of all the modes, while the cavity raises the frequencies of the axisymmetric modes. This eventually helps in setting a pitch which is lower than what is produced by the fundamental. In any case, there is an increased harmonicity when the composite membrane is surrounded by air and even more when it is backed by a cavity.

We now present a detailed investigation of the effect of tension variation on the frequency ratios. Towards this end, we conducted experiments (with the help of a professional tabla player) on a tabla by tuning the frequency of its η_{11} mode to the frequencies of the notes A_4 (440 Hz), B_4^b (466.16 Hz), B_4 (493.88 Hz), and C_5 (523.25 Hz), respectively. Tabla players tune their tablas to the second harmonic by placing their little finger along the diameter at the periphery of the membrane and striking at a point separated by ninety degrees with their index finger. The different modes were excited using the method suggested by Raman.¹ The measurements were taken using an AT2020 USB condenser microphone and the digital signals were analyzed in Matlab environment. Suitable precautions^{2,6} were taken to make sure that the tension in the membrane is as uniform as possible. The results are collected in Table III. We observe that the frequency ratios are all close to integral values except for the last three harmonics which, in general, have only a small contribution in the overall sound of all the major strokes of tabla (this can be confirmed from the spectrums given in Sec. 1.1 of the supplementary material¹²). Second, as expected, the fundamental frequency is not aligned with the other frequencies to form a progressive series of nine harmonically arranged frequencies. It is in fact located about two semi-tones (denoted as *re* in Indian classical music) above the acoustically perceived fundamental (denoted as *sa*). When the player strikes the center of the tabla membrane, what we hear is a sound composed of these two notes

TABLE III. Experimental values of frequency ratios for the right hand tabla at different tuning frequencies.

| Mode | A_4 | B_4^b | B_4 | C_5 |
|-------------|-------|---------|-------|-------|
| η_{01} | 1.156 | 1.128 | 1.122 | 1.122 |
| η_{11} | 2 | 2 | 2 | 2 |
| η_{02} | 2.985 | 2.988 | 2.990 | 3.000 |
| η_{21} | 2.982 | 2.988 | 2.988 | 3.000 |
| η_{12} | 3.969 | 4.03 | 4.027 | 4.025 |
| η_{31} | 3.963 | 4.034 | 4.037 | 4.025 |
| η_{03} | 5.073 | 5.037 | 4.975 | 5.153 |
| η_{22} | 5.063 | 5.068 | 5.012 | 5.148 |
| η_{41} | 5.077 | 5.07 | 4.977 | 5.142 |

(and their harmonics) giving it a chord like flavour, with the tonic and the major-second note. However, in most of the strokes that are typically used, the actual fundamental is suppressed by lightly touching the vibrating membrane giving way to a psychoacoustically perceived fundamental (which is in harmonic relationship with higher frequencies).¹³ Finally, we note that the observations in Table III are consistent with our model which shows remarkable insensitivity to the precise value of tension, given that other parameters are kept fixed.

C. Decay times for the right hand tabla

A distinct feature of tabla is its ability to produce sustained tones with rich harmonic overtones. We can calculate the decay times of various modes using Eq. (12). For a set of parameters, as given in the first row of Table I (except tension), we calculate the decay times for different tension values corresponding to notes A_4 , B_4^b , B_4 , and C_5 . The results are presented in Table IV. The musically important modes (of the kind η_{m1}) clearly have much higher decay times in comparison to other modes. The magnitude of decay times for some of these cases is unreasonably high. This is due to the fact that we have ignored non-radiative dissipative mechanisms and effects of room acoustics from our considerations. That the decay times for $m1$ modes are higher than others is due to the symmetry in the sense that equal amount of area moves in and out of phase during the vibration of the membrane. Also, as expected, the decay times decrease for increasing frequency due to increase in radiative power. We have also calculated the decay times for the case of membrane not backed by an air cavity, noticing that they are then much higher in comparison to the durations obtained for a cavity backed membrane, consistent with the results obtained by Christian *et al.*⁶

D. Frequency ratios and decay times for the left hand tabla

We will now discuss our results for the left hand tabla as idealized in Sec. II B. Our interest again is to investigate the effect of air loading on the acoustics of the drum, in particular with respect to making the frequencies more harmonic and sustaining musically important modes longer than others. To be able to compare our results directly with Ramakrishna,⁴ we take the geometric parameters as

TABLE IV. Mode decay times in seconds. The parameters (except tension) are taken from the first row in Table I.

| Mode | A_4 | B_4^b | B_4 | C_5 |
|-------------|--------|---------|--------|--------|
| η_{01} | 1.8 | 1.7 | 1.5 | 1.3 |
| η_{11} | 26.5 | 22.9 | 18.2 | 14.5 |
| η_{02} | 0.21 | 0.19 | 0.16 | 0.14 |
| η_{21} | 348.2 | 279.8 | 199.0 | 142.1 |
| η_{12} | 0.81 | 0.74 | 0.55 | 0.45 |
| η_{31} | 5800.3 | 4318.2 | 2745.2 | 1755.5 |
| η_{03} | 0.03 | 0.03 | 0.03 | 0.03 |
| η_{22} | 2.4 | 1.9 | 1.4 | 1.0 |

$a = 0.028575$ m, $b = 0.1016$ m, and $d = 0.01905$ m. The frequency ratios are calculated with respect to the frequency of the η_{o11} mode. The length of the air column is taken to be 0.25 m, as measured from an actual tabla. The tension T in the membrane is taken as 3300 N/m, and the density of the loaded patch σ_1 as 0.2 Kg/m², so that we get the most harmonic ratios for the frequencies (see Sec. III E for a discussion on the optimum design parameters). The results are summarized in Table V. It is clear from the table that as we move from the case without any air column to air column just under the loaded patch (i.e., without modified stiffness) to air column under the whole membrane (i.e., with modified air stiffness), the frequency ratios shift close to multiples of 0.5 progressively, except for $\eta_{..02}$. This supports the role of air column in fine tuning the harmonicity of frequencies for the left hand tabla. The decay times for the left hand tabla are clearly much shorter than those for the right hand tabla.

We note that the idealized model for an eccentric composite membrane, as proposed by Ramakrishna⁴ and adapted in Sec. II B, is independent of mass density of either the loading or the base membrane. This assumption is also the reason for the significant difference in certain frequencies when calculated by Ramakrishna with the numerical solutions in Table II of Sathej and Adhkari.³ Although, incorporation of air loading brings forth a dependence on the density of the loaded patch in the model, it will be realistic to develop a framework which includes both the densities.

We have idealized the bowl shaped shell, backing the composite membrane, of the left tabla as a cylinder. Whereas analyzing the effect of non-cylindrical kettle shapes on drum acoustics in a rigorous manner is outside the scope of the present work, we use certain simple arguments to argue that the effect would be insignificant in computing the frequency spectrum. Incorporating a bowl shaped kettle could certainly yield realistic decay rates, but we do not pursue a detailed study here. On the other hand, if we assume the pressure loading to be uniform then the effect of kettle shape is only through the enclosed volume of the cavity and even then only axisymmetric modes are to be affected. A simple analytical formulation¹⁷ could then

TABLE V. Frequency ratios and decay times for the left hand tabla, with $a = 0.028575$ m, $b = 0.1016$ m, $d = 0.01905$ m, $L = 0.25$ m, $\sigma_1 = 0.2$ Kg/m², and $T = 3300$ N/m.

| Mode | Without air column (Ref. 4) | Air column without modified stiffness | Air column with modified stiffness | Decay time (s) |
|---------------|-----------------------------|---------------------------------------|------------------------------------|----------------|
| $\eta_{..01}$ | 0.49 | 0.49 | 0.50 | 0.017 |
| η_{e11} | 0.97 | 0.97 | 0.97 | 0.066 |
| η_{o11} | 1.00 | 1.00 | 1.00 | 0.068 |
| η_{e21} | 1.46 | 1.51 | 1.50 | 0.326 |
| η_{o21} | 1.47 | 1.52 | 1.51 | 0.33 |
| $\eta_{..02}$ | 1.72 | 1.80 | 1.77 | 0.35 |
| η_{e31} | 1.94 | 2.03 | 2.00 | 1.22 |
| η_{o31} | 1.95 | 2.03 | 2.00 | 1.23 |
| η_{e12} | 2.34 | 2.46 | 2.42 | 0.18 |
| η_{o12} | 2.35 | 2.47 | 2.43 | 0.18 |

be used to obtain frequency spectrums for various shapes with fixed radius and height. We observed that between kettles of cylindrical, paraboloid, and a cylinder cupped by a hemisphere shape there is little difference in the frequency values. Similar conclusion was also reached in the doctoral work of Davis,¹⁸ for the case of timpani. Finally, following Rossing,¹⁹ we observe that the sound wavelengths are much larger than the kettle dimensions and therefore the modal frequencies should remain mostly unaffected by the choice of kettle shape.

E. Optimal design for left hand tabla

We fix the length of the air column to be 0.25 m, as measured from an actual tabla. We also fix other geometrical parameters, as given above, and postulate an error function

$$E_l(\sigma_1, T) = \left(\frac{\omega_{e1}/\omega_{o11} - 0.5}{0.5} \right)^2 + \left(\frac{\omega_{e11}/\omega_{o11} - 1}{1} \right)^2 + \left(\frac{\omega_{e21}/\omega_{o11} - 1.5}{1.5} \right)^2 + \left(\frac{\omega_{o21}/\omega_{o11} - 1.5}{1.5} \right)^2 + \left(\frac{\omega_{e31}/\omega_{o11} - 2}{2} \right)^2 + \left(\frac{\omega_{o31}/\omega_{o11} - 2}{2} \right)^2 + \left(\frac{\omega_{e12}/\omega_{o11} - 2.5}{2.5} \right)^2 + \left(\frac{\omega_{o12}/\omega_{o11} - 2.5}{2.5} \right)^2 \quad (25)$$

in terms of two free parameters: density of the loaded patch σ_1 and tension T in the membrane. The form of the error function is motivated from the results obtained in Sec. III D. To get the most harmonic ratios for the frequencies, we vary the two parameters over a suitable range and seek their value which minimizes the error function. From the contour plot of E_l , in Fig. 5, it is clear that E_l has a flat valley around the minima and therefore there are possibly a large number of parameter values which yield close to optimum results. For our calculations in the preceding section we choose $(\sigma_1, T) = (0.2 \text{ Kg/m}^2, 3300 \text{ N/m})$ so as to remain close to values for an actual tabla. The error values corresponding to the three cases in Table V are then obtained as 0.0116,

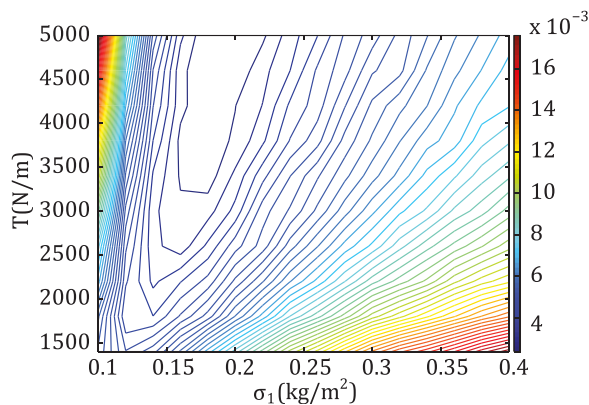


FIG. 5. (Color online) Contour plots for the error function corresponding to the left hand tabla.

0.0025, and 0.0027. As expected, error is minimized by an order or magnitude by incorporating air pressure. Notably, the error is close for cases when air pressure is considered just below the loaded patch and below the whole membrane.

F. Modal sound synthesis

An appropriate methodology for numerical sound synthesis of tabla sounds can be an extremely useful step towards digitizing Indian percussion sounds. In this section, we apply modal sound synthesis technique to synthesize tabla sounds. The modal synthesis is performed on the basis of modes with complex frequencies obtained from solving the physical model.²⁰ For the purpose of the present analysis, we will use the modes and their frequencies as obtained in the above sections for both the tablas. The details of our numerical calculation are given in Secs. 1 and 2 of the supplementary material.¹²

We perform modal analysis of tabla membranes subjecting them to an initial velocity represented by a “raised cosine profile” simulating a snap stroke at a point on the tabla.²⁰ In order to compare the obtained velocity evolution for the right hand tabla with experimental results, we choose the parameters as given in the first row of Table I except for tension, which is chosen so as to match the fundamental frequency with the obtained fundamental frequency from *tin* stroke (see Sec. 1.1 in the supplementary material¹² for more details on the nature of this tabla stroke). We then pick a point on the membrane, find its velocity with respect to time over a large time interval and a sufficiently large value of sampling frequency. We take fast Fourier transform of the temporal velocity value over the time interval and compare it with the experimentally obtained spectrums. Different strokes can be simulated by varying the position of the initial velocity field and by removing unwanted modes (which are otherwise suppressed by placing fingers on the edge of the membrane). Figures 6(a) and 6(b) show the frequency spectrums for *tin* and *nā* strokes as obtained from the sound

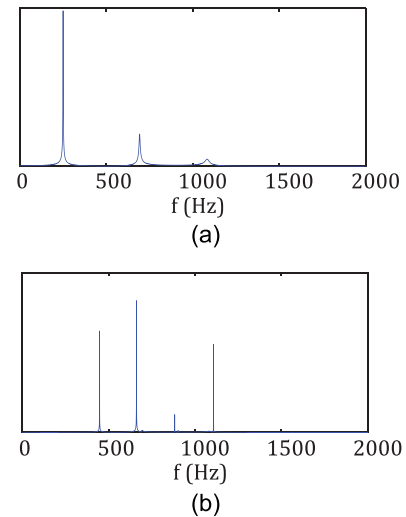


FIG. 6. (Color online) Frequency spectrums corresponding to *tin* and *nā* strokes as obtained from the modal sound synthesis of the right hand tabla.

synthesis. Further details, including time variations of displacement at an arbitrary point, are given in the supplementary material.¹² The stroke *tin* consists of a thump at the center of the black patch whereas *nā* is generated by striking at the edge of the membrane, using only the index finger, and keeping out the fundamental mode. The obtained spectrums are in good agreement with the corresponding experimental recordings (provided in the supplementary material¹²). The modal sound synthesis for the left hand tabla can be performed similarly. Some preliminary results towards that end are included in Sec. 2 of the supplementary material.¹²

IV. CONCLUDING REMARKS

There are several drums in the Indian musical tradition which convey a strong sense of pitch. Many of these now belong to antiquity and are present today only in archeological remains and old musicology texts.^{21,22} Among the extant drums which produce rich harmonic overtones are *pakhāvaj*, *mridangam*, and tabla, all of which have composite membranes (loaded with additional mass in a small region) backed by air cavity. There are others, like hourglass shaped drums *damru* and *uddukku*, which convey strong pitch as a result of skilful variation of tension in the drumhead while playing the drum.^{22,23} Interestingly, *uddukku*, which is a temple drum from the southern Indian state of Kerela, is strikingly similar to African talking drums and Japanese *tsuzumi*. Our study of tabla can be extended to barrel drums like *pakhāvaj* and *mridangam*, where two composite drumheads are attached to opposite sides of a barrel shaped shell. The two drumheads in these barrel drums are of different sizes and are loaded differently.^{21,22} The acoustical study of tabla can be furthered by investigating the appropriateness of the paste material for mass loading, nature of animal hide used, and type of wood suitable for the shell. The tabla makers are usually very rigid about the choice of materials used for tabla making.¹⁰ On the other hand, more realistic boundary conditions for pressure can be used to model, for example, the substantial roughness that is introduced in the interior of the shell while hollowing out the right hand tabla.

ACKNOWLEDGMENT

We are grateful to Professor Anindya Chatterjee, Professor Shakti Singh Gupta, and Professor Sovan Das for their valuable comments. We thank Mohit Kumar, a professional tabla player, for helping us in our experiments. We are thankful to the anonymous referees for their useful comments, in particular for bringing to our attention the work done in an unpublished master's thesis.⁸

APPENDIX A: EIGENFUNCTIONS FOR THE RIGHT HAND TABLA

The eigenfunctions η^0 's for the composite membrane of the right hand tabla, without air loading, are given by²

$$\eta_{1mn}^0(\rho, \phi) = A_{mn} J_m(\lambda k X_{mn} \rho / a) e^{im\phi} \quad \text{for } 0 \leq \rho \leq a, \text{ and} \quad (\text{A1})$$

$$\eta_{2mn}^0(\rho, \phi) = A_{mn} \frac{J_m(\lambda k X_{mn})}{J_m(k X_{mn}) Y_m(X_{mn}) - J_m(X_{mn}) Y_m(k X_{mn})} \left[J_m\left(\frac{X_{mn} \rho}{b}\right) Y_m(X_{mn}) - J_m(X_{mn}) Y_m\left(\frac{X_{mn} \rho}{b}\right) \right] e^{im\phi} \quad (\text{A2})$$

for $a < \rho \leq b$. In these expressions, $k = a/b$, $\lambda^2 = \sigma_1/\sigma_2$, and $X_{mn} = \omega_{mn}^0 b/c_2$ is the n th root of

$$\lambda \frac{J_{m-1}(\lambda k X)}{J_m(\lambda k X)} = \frac{J_{m-1}(k X) Y_m(X) - J_m(X) Y_{m-1}(k X)}{J_m(k X) Y_m(X) - J_m(X) Y_m(k X)}, \quad (\text{A3})$$

$c_2 = \sqrt{T/\sigma_2}$ being the speed of transverse waves in the unloaded region and ω_{mn}^0 the natural frequencies of transverse vibrations of the unloaded membrane.

APPENDIX B: EXPRESSIONS FOR $U_{nn'}$ AND $V_{nn'}$

$$\begin{aligned} U_{nn'} &= \frac{1}{4\pi} \int_0^a \int_0^{2\pi} \int_0^a \rho' d\rho' \int_0^{2\pi} d\phi' G_{\text{in}}(\rho, \phi, L-|\rho', \phi', L) \eta_{1mn'}^0(\rho', \phi') \eta_{1mn}^0(\rho, \phi) \rho d\phi d\rho \\ &+ \frac{1}{4\pi} \int_0^a \int_0^{2\pi} \int_a^b \rho' d\rho' \int_0^{2\pi} d\phi' G_{\text{in}}(\rho, \phi, L-|\rho', \phi', L) \eta_{2mn'}^0(\rho', \phi') \eta_{1mn}^0(\rho, \phi) \rho d\phi d\rho \\ &+ \frac{1}{4\pi} \int_a^b \int_0^{2\pi} \int_0^a \rho' d\rho' \int_0^{2\pi} d\phi' G_{\text{in}}(\rho, \phi, L-|\rho', \phi', L) \eta_{1mn'}^0(\rho', \phi') \eta_{2mn}^0(\rho, \phi) \rho d\phi d\rho \\ &+ \frac{1}{4\pi} \int_a^b \int_0^{2\pi} \int_a^b \rho' d\rho' \int_0^{2\pi} d\phi' G_{\text{in}}(\rho, \phi, L-|\rho', \phi', L) \eta_{2mn'}^0(\rho', \phi') \eta_{2mn}^0(\rho, \phi) \rho d\phi d\rho, \end{aligned} \quad (\text{B1})$$

$$\begin{aligned}
V_{nn''} = & \frac{1}{4\pi} \int_0^a \int_0^{2\pi} \int_0^a \rho' d\rho' \int_0^{2\pi} d\phi' G_{\text{out}}(\rho, \phi, L_+ | \rho', \phi', L) \eta_{1mn''}^0(\rho', \phi') \eta_{1mn}^0(\rho, \phi) \rho d\phi d\rho \\
& + \frac{1}{4\pi} \int_0^a \int_0^{2\pi} \int_a^b \rho' d\rho' \int_0^{2\pi} d\phi' G_{\text{out}}(\rho, \phi, L_+ | \rho', \phi', L) \eta_{2mn''}^0(\rho', \phi') \eta_{1mn}^0(\rho, \phi) \rho d\phi d\rho \\
& + \frac{1}{4\pi} \int_a^b \int_0^{2\pi} \int_0^a \rho' d\rho' \int_0^{2\pi} d\phi' G_{\text{out}}(\rho, \phi, L_+ | \rho', \phi', L) \eta_{1mn''}^0(\rho', \phi') \eta_{2mn}^0(\rho, \phi) \rho d\phi d\rho \\
& + \frac{1}{4\pi} \int_a^b \int_0^{2\pi} \int_a^b \rho' d\rho' \int_0^{2\pi} d\phi' G_{\text{out}}(\rho, \phi, L_+ | \rho', \phi', L) \eta_{2mn''}^0(\rho', \phi') \eta_{2mn}^0(\rho, \phi) \rho d\phi d\rho.
\end{aligned} \tag{B2}$$

In these expressions,

$$\begin{aligned}
G_{\text{in}}(\rho, \phi, z | \rho', \phi', z') \\
= & -4\pi \sum_{m=-\infty}^{\infty} \frac{e^{im(\phi-\phi')}}{2\pi} \\
& \times \sum_{n=1}^{\infty} \frac{2J_m[y_{mn}(\rho/b)]J_m[y_{mn}(\rho'/b)]}{b^2(1-m^2/y_{mn}^2)J_m^2(y_{mn})} \\
& \times \frac{\cos[\gamma_{mn}z] \cos[\gamma_{mn}(L-z)]}{\gamma_{mn} \sin(\gamma_{mn}L)},
\end{aligned} \tag{B3}$$

where y_{mn} is the solution of $J_m'(y_{mn}) = 0$, $z_>$, $z_<$ denote the greater and lesser of z and z' , respectively, and

$$\begin{aligned}
\gamma_{mn} = & \sqrt{\omega^2/c_a^2 - y_{mn}^2/b^2} \quad \text{for } y_{mn} < \omega b/c_a, \\
\gamma_{mn} = & i\sqrt{y_{mn}^2/b^2 - \omega^2/c_a^2} \quad \text{for } y_{mn} > \omega b/c_a.
\end{aligned} \tag{B4}$$

Also

$$\begin{aligned}
G_{\text{out}}(\rho, \phi, z | \rho', \phi', z') \\
= & \frac{e^{i(\omega/c_a)\sqrt{\rho^2+\rho'^2-2\rho\rho'\cos(\phi-\phi')+(z-z')^2}}}{\sqrt{\rho^2+\rho'^2-2\rho\rho'\cos(\phi-\phi')+(z-z')^2}} \\
& + \frac{e^{i(\omega/c_a)\sqrt{\rho^2+\rho'^2-2\rho\rho'\cos(\phi-\phi')+(z+z'-2L)^2}}}{\sqrt{\rho^2+\rho'^2-2\rho\rho'\cos(\phi-\phi')+(z+z'-2L)^2}}.
\end{aligned} \tag{B5}$$

¹C. V. Raman, "The Indian musical drums," Proc. Indian Acad. Sci., Sect. A **1**, 179–188 (1934).

²B. S. Ramakrishna and M. M. Sondhi, "Vibrations of Indian musical drums regarded as composite membranes," J. Acoust. Soc. Am. **26**, 523–529 (1954).

³G. Sathej and R. Adhikari, "The eigenspectra of Indian musical drums," J. Acoust. Soc. Am. **125**, 831–838 (2009).

⁴B. S. Ramakrishna, "Modes of vibration of the Indian drum dugga or left-hand thabala," J. Acoust. Soc. Am. **29**, 234–238 (1957).

⁵T. D. Rossing, "The physics of kettledrums," Sci. Am. **247**, 172–178 (1982).

⁶R. S. Christian, R. E. Davis, A. Tubis, C. A. Anderson, R. I. Mills, and T. D. Rossing, "Effect of air loading on timpani membrane vibrations," J. Acoust. Soc. Am. **76**, 1336–1345 (1984).

⁷R. B. Bhat, "Acoustics of a cavity-backed membrane: The Indian musical drum," J. Acoust. Soc. Am. **90**, 1469–1474 (1991).

⁸G. Saraswat, "Indian musical drum eigenspectra and sound synthesis," M. Tech. thesis IIT Madras, 2011.

⁹J. Kippen, *The Tabla of Lucknow: A Cultural Analysis of a Musical Tradition* (Manohar, New Delhi, 2005), pp. xvi–xvii and 145–149.

¹⁰P. A. Roda, "Resounding objects: Musical materialities and the making of banarasi tablas," Ph.D. thesis, New York University, 2013.

¹¹B. M. Banerjee and D. Nag, "The acoustical character of sounds from Indian twin drums," Acustica **75**, 206–208 (1991).

¹²See supplementary material at <http://dx.doi.org/10.1121/1.4979782> for further details on modal sound synthesis and additional results on optimization.

¹³D. Courtney, "Psychoacoustics of the musical pitch of tabla," J. Sangeet Res. Acad. **13**, 9–13 (1999).

¹⁴T. Sarojini and A. Rahman, "Variational method for the vibrations of the Indian drums," J. Acoust. Soc. Am. **30**, 191–196 (1958).

¹⁵S. De, "Experimental study of the vibration characteristics of a loaded kettledrum," Acustica **40**, 206–210 (1978).

¹⁶S. Gaudet, C. Gauthier, and S. Léger "The evolution of harmonic Indian musical drums: A mathematical perspective," J. Sound Vib. **291**, 388–394 (2006).

¹⁷P. M. Morse, *Vibration and Sound* (McGraw-Hill, New York, 1948), pp. 193–195.

¹⁸R. E. Davis, "Mathematical modeling of the orchestral timpani," Ph.D. thesis, Purdue University, 1988.

¹⁹T. D. Rossing, *Science of Percussion Instruments* (World Scientific, Singapore, 2000), p. 12.

²⁰S. Bilbao, *Numerical Sound Synthesis* (Wiley, West Sussex, UK, 2009), Chaps. 1 and 11.

²¹B. C. Deva, *Musical Instruments of India* (Firma KLM Private Limited, Calcutta, 1978), Chap. VI.

²²L. Mishra, *Bharatiya Sangeet Vaadya* (Bharatiya Jnanpith, New Delhi, 2002), pp. 143–213.

²³L. S. Rajagopalan, *Temple Musical Instruments of Kerala* (Sangeet Natak Akademi, New Delhi, 2010), Chap. 1.